

Supporting Information

Cell-Selective Cytotoxicity of a Fluorescent Rhodium Metalloinsertor Conjugate Results from Irreversible DNA Damage at Base Pair Mismatches

*Adela Nano,^{†#} Julie M. Bailis,^{‡**} Natalie F. Mariano,[‡] Elizabeth D. Pham,[‡] Stephanie D.
Threatt,[†] and Jacqueline K. Barton^{†*}*

[†] Division of Chemistry and Chemical Engineering, California Institute of Technology,
Pasadena, CA 91125

[‡] Department of Oncology Research, Amgen Research, Amgen, Inc., South San Francisco, CA
94080

[#] These authors contributed equally to the work.

* To whom correspondence should be addressed. Julie M. Bailis, Email: jbailis@amgen.com;

Telephone: +1 (650) 244 2361, and Jacqueline K. Barton, Email: jkbarton@caltech.edu;

Telephone: +1 (626) 395-6075; Fax: +1 (626) 577-4976.

Table of Figures

Figure S1. ^1H NMR spectrum of RhDPA-Cy3.	3
Figure S2. ^{13}C NMR spectrum of RhDPA-Cy3.	3
Figure S3. ^1H NMR spectrum of RhPPO-Cy3.	4
Figure S4. TOF-MS ES+ characterization of RhDPA-Cy3.	5
Figure S5. TOF-MS ES+ characterization of RhPPO-Cy3.	6
Figure S6. MS-ESI+ characterization of RhPPO-Cy3 using an LTQ spectrometer.	7
Figure S7. HPLC trace of RhPPO-Cy3 after purification.	8
Figure S8. Absorption profile of RhPPO-Cy3, and its models Cy3-linker and RhPPO-Hdpa.	9
Figure S9. Evaluation of cytotoxicity of RhPPO-Cy3 at different time points.	10
Figure S10. RhPPO-Cy3 shows preferential cytotoxicity for MMR-deficient CRC cell lines.	11
Figure S11. RhPPO-Cy3 causes DNA damage.	12

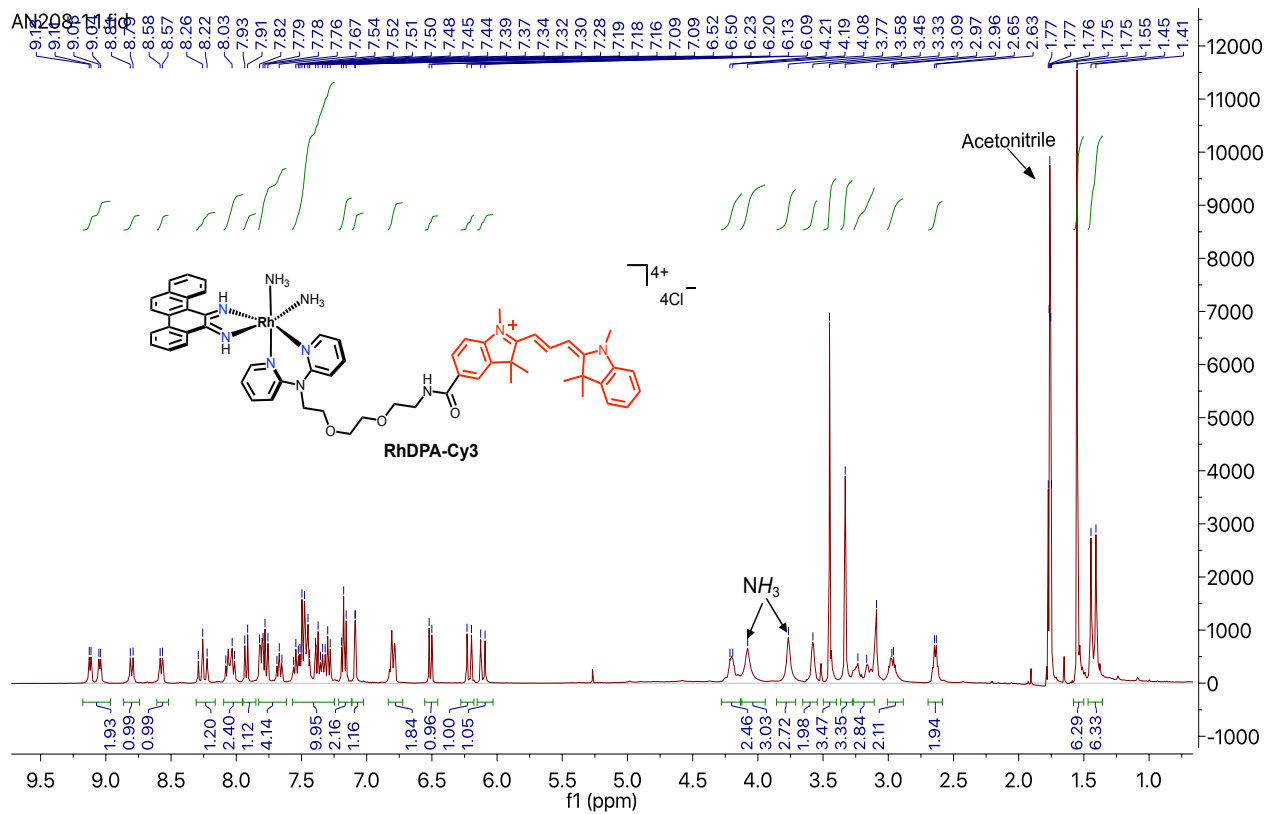


Figure S1. ^1H NMR spectrum of RhDPA-Cy3. The spectrum was collected in deuterated acetonitrile at room temperature.

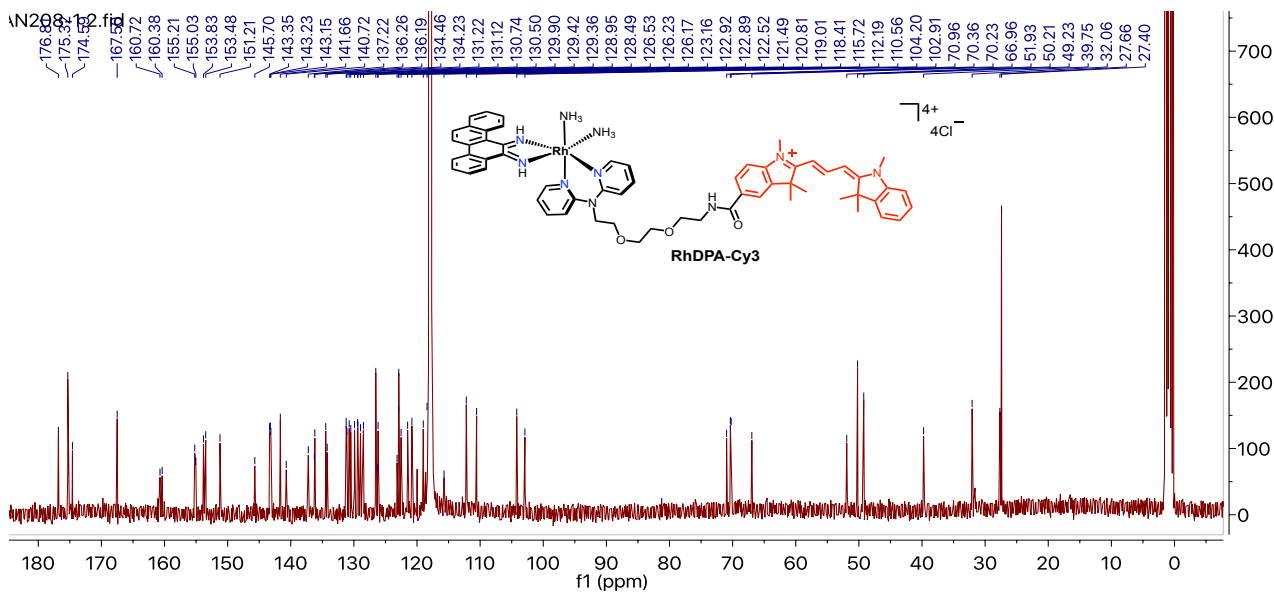


Figure S2. ^{13}C NMR spectrum of RhDPA-Cy3. The spectrum was collected in deuterated acetonitrile at room temperature.

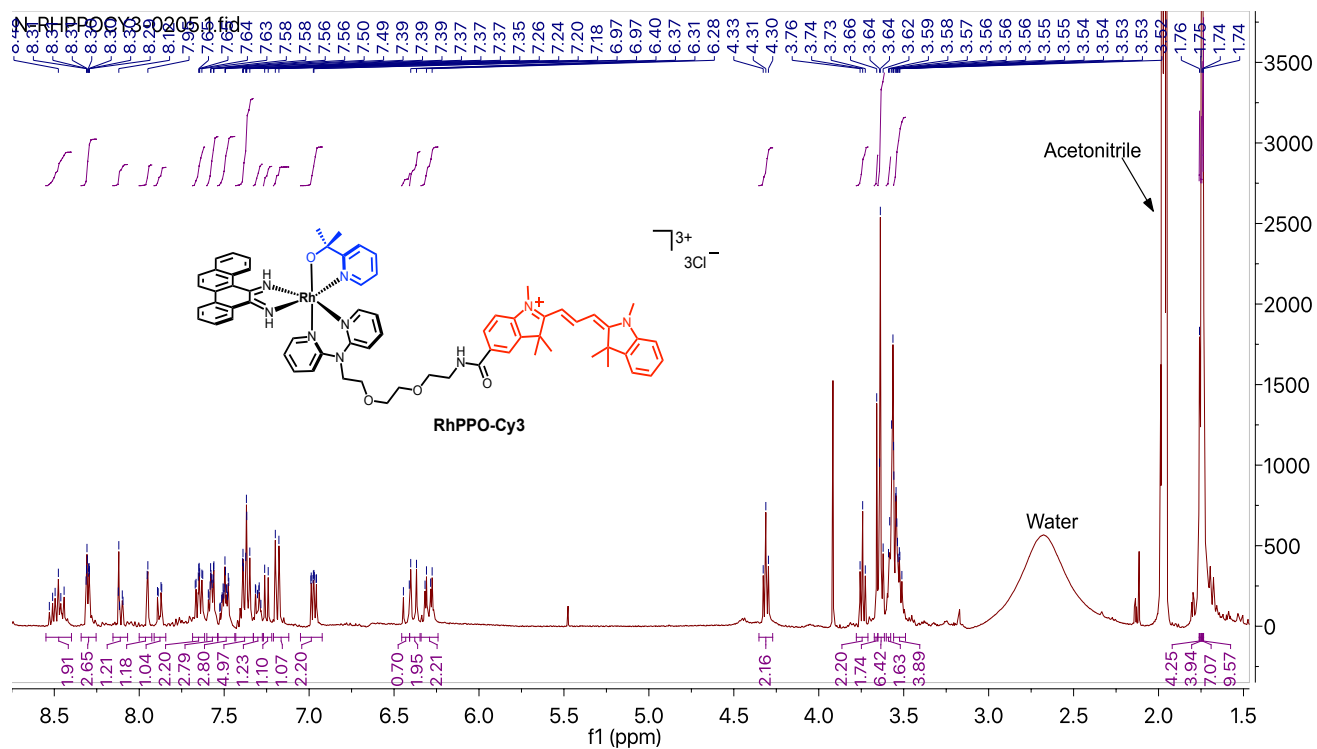


Figure S3. ^{13}H NMR spectrum of RhPPO-Cy3. The spectrum was collected in deuterated acetonitrile at room temperature. The compound was obtained as a diastereomeric mixture and characterized as such.

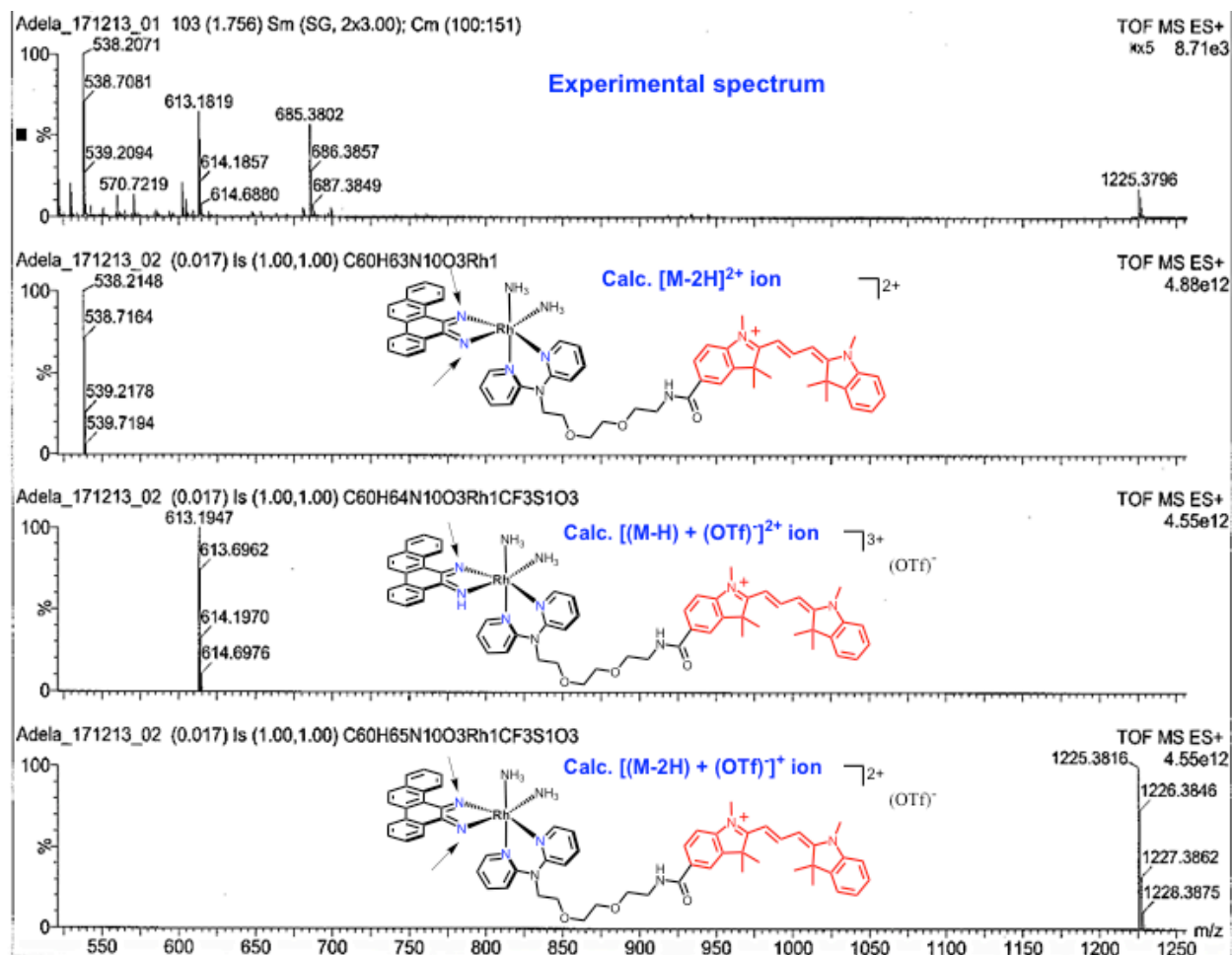


Figure S4. TOF-MS ES⁺ characterization of RhDPA-Cy₃. (Upper) Experimental spectrum of RhDPA-Cy₃; (Lower) Calculated spectra for *m/z* 538.2; 613.1; 1225.3. When the spectrum was recorded, the compound was not anion exchanged to its chloride salt. Therefore, we observe the triflate salt in the experimental spectrum.

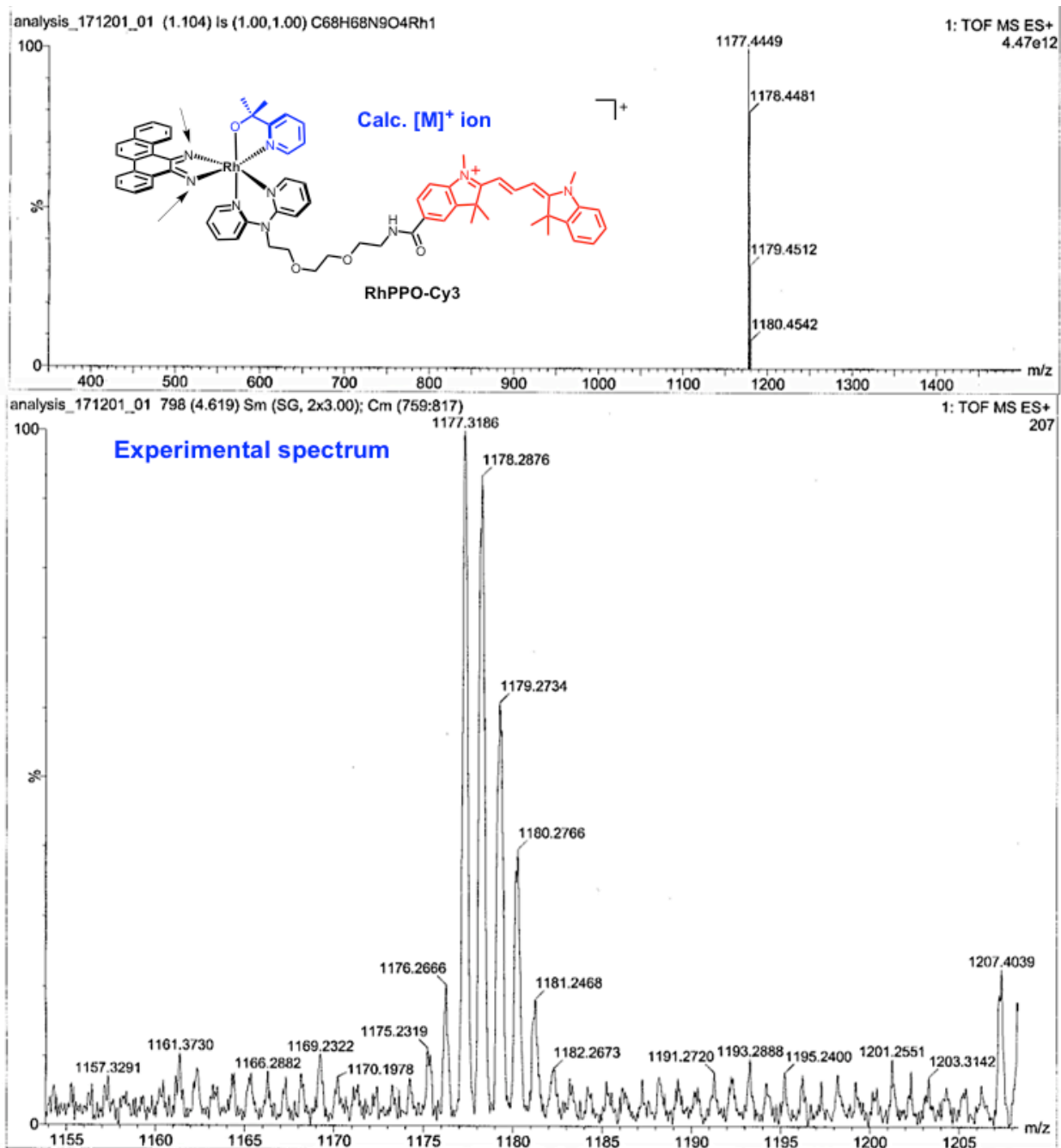


Figure S5. TOF-MS ES⁺ characterization of RhPPO-Cy3. (Upper) Calculated $m/z = 1177.4449$ for $[M - 2H]^+$; (Lower) Experimental spectrum with $m/z = 1177.3186$. $[M - 2H]^+$ is assigned to the complex with both imines deprotonated, indicated with an arrow in the chemical structure.

rhppocy-hplc-30_180731215207 #1-20 RT: 0.00-0.07 AV: 20 NL: 9.46E5
T: ITMS + p ESI Full ms [150.00-2000.00]

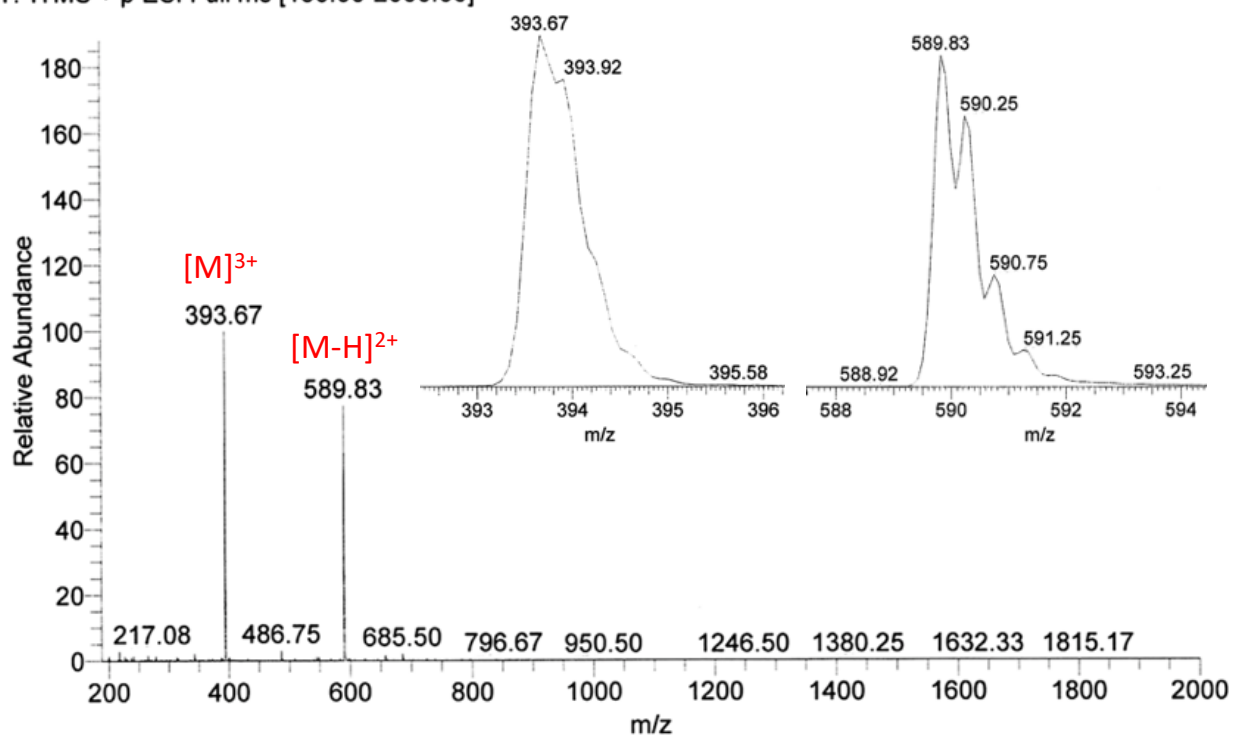


Figure S6. MS-ESI+ characterization of RhPPO-Cy3 using an LTQ spectrometer. The spectrum was recorded after HPLC purification of RhPPO-Cy3. Insets are zooms of m/z 393.67 and m/z 589.83 peak; m/z 393.67 (100%) corresponds to $[M]^{3+}$ (both imines on chrysi ligand are protonated); m/z 589.83 (77%) corresponds to $[M - H]^{2+}$ (only one imine is protonated).

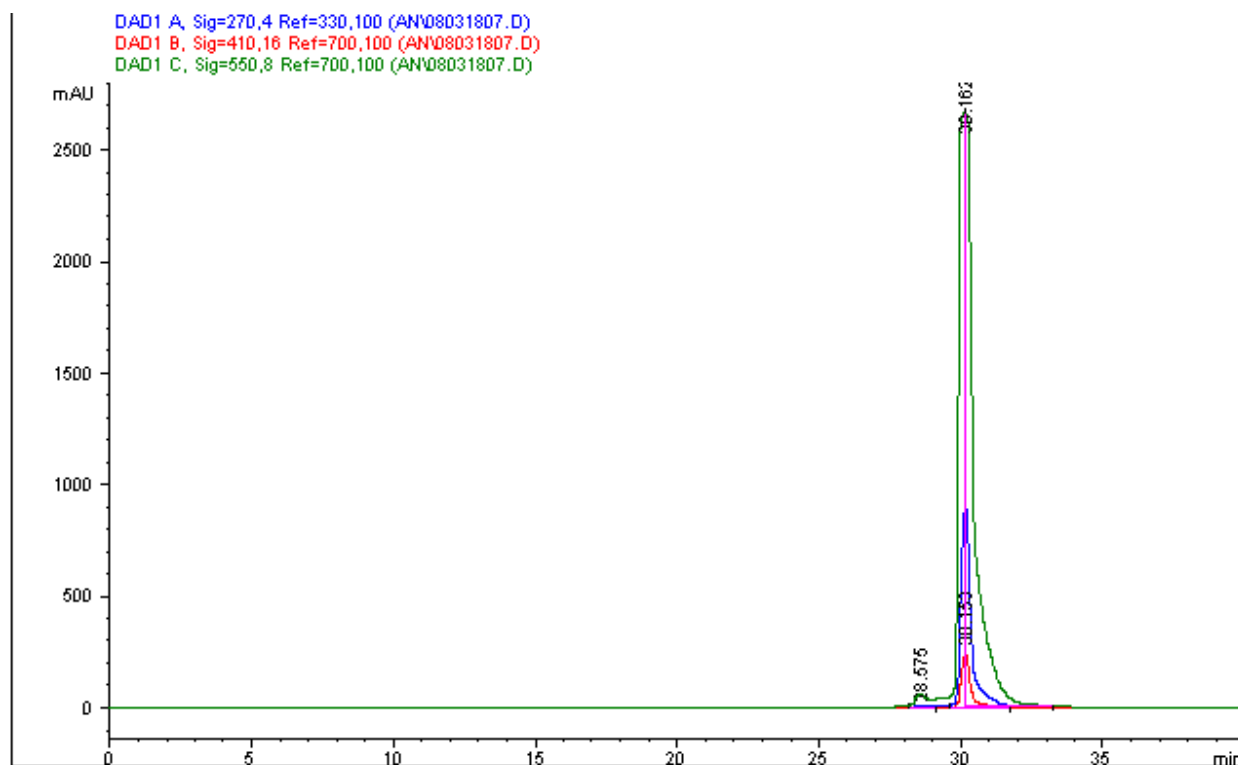


Figure S7. HPLC trace of RhPPO-Cy3 after purification. The HPLC purification was followed using three different wavelengths: at 270 nm, 410 nm (marking the absorption of rhodium complex center), and 550 nm (marking the absorption of Cy3 dye). Mobile phase: 85/15 to 50/50 to 85/50 (0.1% trifluoroacetic acid in water)/acetonitrile eluting over 40 minutes.

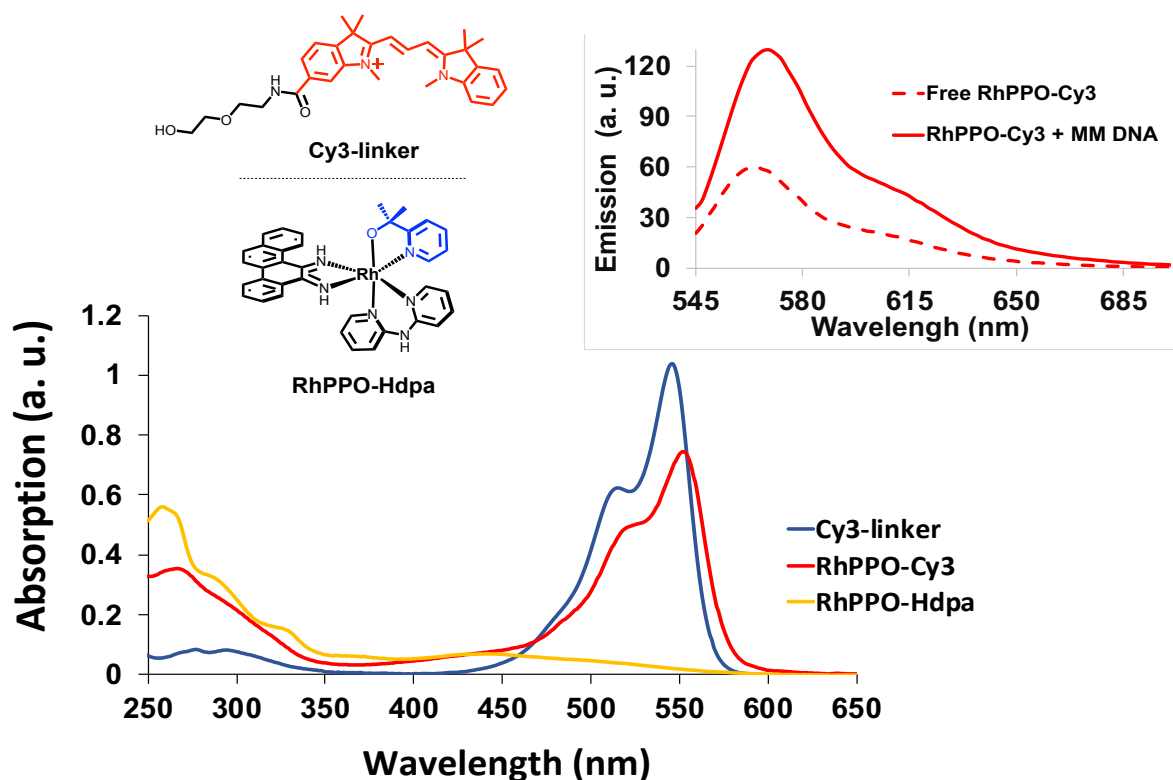


Figure S8. Absorption profile of RhPPO-Cy3, and its models Cy3-linker and RhPPO-Hdpa. Spectra collected in Tris buffer (5mM Tris, 200 mM NaCl, pH 7.4) at room temperature. [RhPPO-Cy3]; [Cy3-linker]; [RhPPO-Hdpa] = 10 μ M. Absorption maxima for RhPPO-Cy3 (in Tris 5 mM, 200 mM NaCl, pH 7.4): $\lambda(552\text{nm}) \epsilon = 61,000 \text{ M}^{-1} \text{ cm}^{-1}$; $\lambda(267\text{nm}) \epsilon = 28,000 \text{ M}^{-1} \text{ cm}^{-1}$. Inset: Emission of RhPPO-Cy3 at 1 μ M free in Tris buffer solution (5mM Tris, 200 mM NaCl, pH 7.4) with $\lambda_{\text{max}} = 565 \text{ nm}$, or in the presence of 1 eq. MM dsDNA with $\lambda_{\text{max}} = 570 \text{ nm}$. The synthesis and characterization of RhPPO-Hdpa and Cy3-linker have been previously reported.^{1,2}

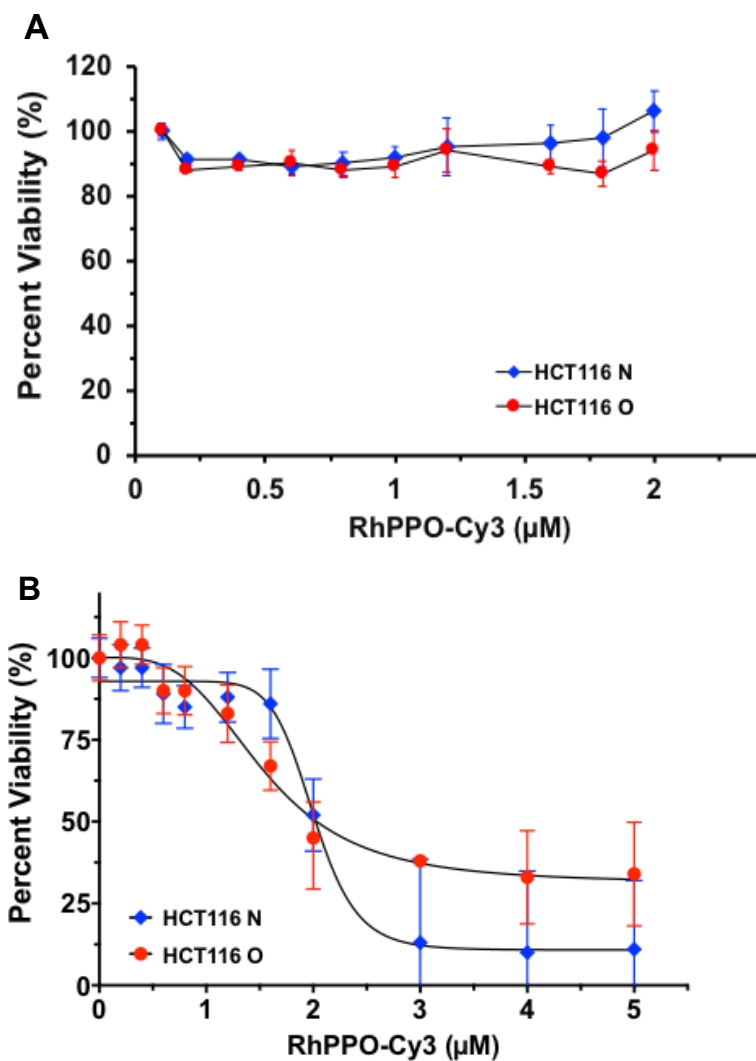


Figure S9. Evaluation of cytotoxicity of RhPPO-Cy3 at different time points. The cells were treated with RhPPO-Cy3 at the concentrations indicated, and then cell viability was assessed with a Cell Titer-glo assay. (A) Dose response curve of cell viability assessed after 24 hours incubation with RhPPO-Cy3; (B) dose response curve assessed after 48 hours incubation with RhPPO-Cy3. Error bars are representative of three replicates.

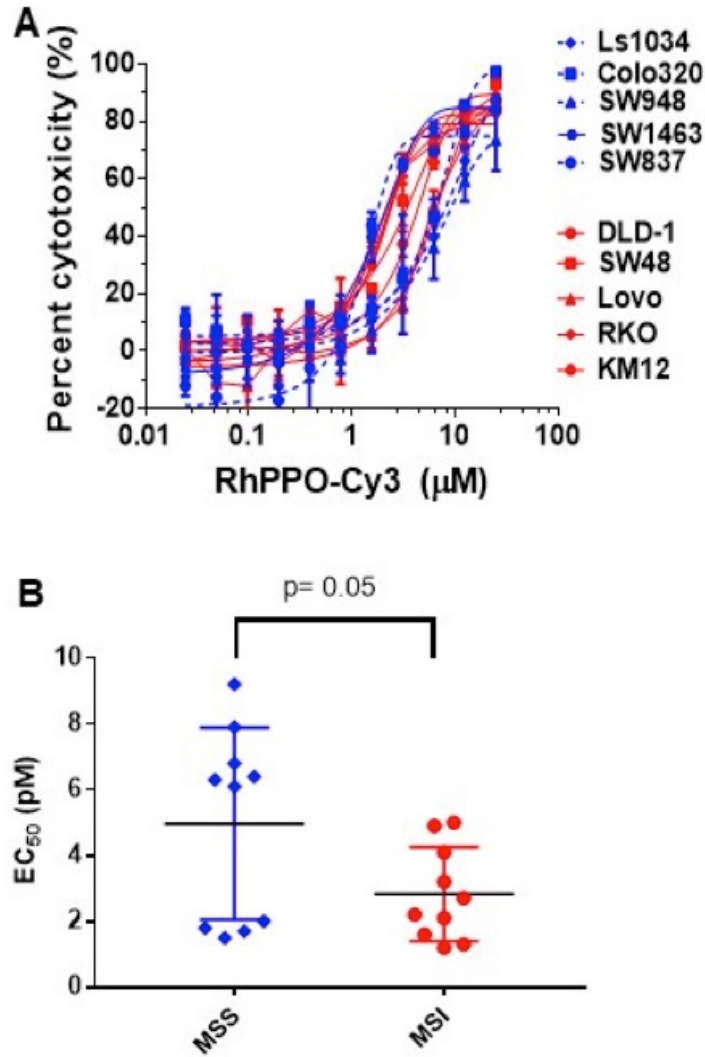


Figure S10. RhPPO-Cy3 shows preferential cytotoxicity for MMR-deficient CRC cell lines. A panel of MMR-deficient and MMR-proficient CRC cell lines was treated with RhPPO-Cy3 in a dose response. After 72 hours incubation, cell viability was assessed with a Cell Titer-glo assay. Duplicate samples were analyzed in each experiment. (A) Dose response curves from a representative experiment are shown. In blue are MSS cell lines; in red are MSI cell lines. (B) Comparison of EC_{50} values for the MSS and MSI cell lines.

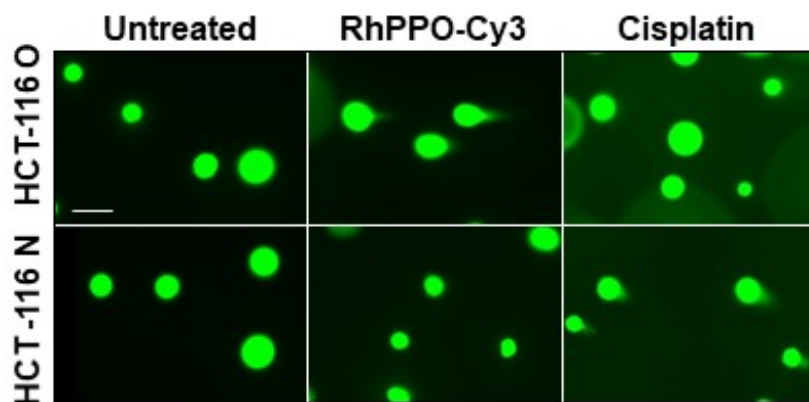


Figure S11. RhPPO-Cy3 causes DNA damage. HCT-116 O and HCT-116 N cells were treated with 5 μ M RhPPO-Cy3 or cisplatin for 24 hours, and then analyzed for DNA damage using a neutral Comet assay. Cells were embedded in agarose, denatured and analyzed by TBE gel electrophoresis. Cell nuclei and comet tails were visualized with a Vista Green fluorescent dye. Representative images are shown. Scale bar, 20 μ M.

REFERENCES

1. Boyle, K. M.; Barton, J. K. (2018) A Family of Rhodium Complexes with Selective Toxicity toward Mismatch Repair-Deficient Cancers. *J. Am. Chem. Soc.* *140*, 5612-5624.
2. Nano, A.; Boynton, A.; Barton, J.K. (2017) A Rhodium-Cyanine Fluorescent Probe: Detection and Signaling of Mismatches in DNA. *J. Am. Chem. Soc.* *139*, 17301-17304.